

RESEARCH

Open Access



The correlation analysis between Normalized Wall Index and cerebral perfusion in patients with Mild Carotid Artery Stenosis under 3.0T MRI

Yonggang Cai¹, Shouming Chen^{1*}, Tongyu Shang¹, Binze Han¹, Lei Zhang¹, Changyan Xu¹, Zhibin He¹ and Ting Yin¹

Abstract

Background To explore the relationship between Normalized Wall Index (NWI) and Magnetic Resonance Perfusion Imaging Parameters in Patients with Mild Carotid Artery Stenosis.

Methods Initially, an analysis was conducted on 40 patients from our institution, and we identified through ultrasonographic examinations conducted between July 2021 and August 2022. These patients exhibited carotid artery plaques with mild luminal narrowing (with stenosis rates ranging from 20 to 50%, following the criteria of the North American Symptomatic Carotid Endarterectomy Trial, NASCET). All cases underwent high-resolution magnetic resonance imaging (MRI) of the carotid arteries and cerebral perfusion assessments using 3.0T MRI during the specified timeframe. Based on whether the cerebral hemisphere in the carotid artery supply region had experienced ischemic events, including Transient Ischemic Attacks (TIAs), patients were categorized into symptomatic and asymptomatic groups. Subsequently, the Normalized Wall Index (NWI) of the carotid arteries and the area of abnormal perfusion on the same side of the brain were calculated for each group.

Results In the symptomatic group, all patients exhibited perfusion abnormalities in the internal carotid artery supply region, whereas only some patients in the asymptomatic group showed such abnormalities. The NWI of plaques in the symptomatic group was significantly higher than that in the asymptomatic group ($P < 0.05$).

Conclusion The range of prolongation in mean transit time (MTT) and time to peak (TTP) in patients with perfusion abnormalities was positively correlated with NWI and stenosis rates. The association with NWI was more pronounced and statistically significant ($P < 0.05$).

Keywords High-resolution magnetic resonance vessel wall imaging, Carotid artery plaques, Cerebral perfusion, Cerebrovascular events, Luminal narrowing, Normalized wall index

*Correspondence:

Shouming Chen
chenshouming2024@yeah.net

¹Imaging Center, Affiliated Hospital of Panzhihua University, No. 27, Taoyuan Street, East District, Panzhihua City, Sichuan Province, China



© The Author(s) 2025. **Open Access** This article is licensed under a Creative Commons Attribution-NonCommercial-NoDerivatives 4.0 International License, which permits any non-commercial use, sharing, distribution and reproduction in any medium or format, as long as you give appropriate credit to the original author(s) and the source, provide a link to the Creative Commons licence, and indicate if you modified the licensed material. You do not have permission under this licence to share adapted material derived from this article or parts of it. The images or other third party material in this article are included in the article's Creative Commons licence, unless indicated otherwise in a credit line to the material. If material is not included in the article's Creative Commons licence and your intended use is not permitted by statutory regulation or exceeds the permitted use, you will need to obtain permission directly from the copyright holder. To view a copy of this licence, visit <http://creativecommons.org/licenses/by-nc-nd/4.0/>.

Introduction

Carotid atherosclerotic plaques are closely associated with ischemic stroke, and unstable plaques are a major cause of acute ischemic stroke. Based on compositional features such as intraplaque hemorrhage (IPH), plaque rupture, neovascularization within the plaque, fibrous cap thickness, and lipid-rich necrotic core (LRNC), these imaging characteristics are used for risk stratification [1]. Utilizing high-field MRI equipment, dedicated head-neck coils, and multi-sequence scanning techniques not only allows for the detection of plaque composition but also facilitates the observation of changes in vascular wall morphology and wall stress. This approach provides accurate information regarding plaque size, volume, and vulnerability. Currently, MRI is recognized as the optimal method for quantitative measurement of carotid artery plaque burden and non-invasive assessment of plaque composition [2]. It enables precise measurements of plaque burden, including vessel area (VA), lumen area (LA), maximum wall thickness (maxWT), Normalized Wall Index (NWI), and other indicators, with good interobserver measurement consistency.

In clinical practice, the majority of treatments for cerebral ischemic changes are initiated after the occurrence of ischemic clinical symptoms. Therefore, early radiological assessment of carotid artery plaques and their associated risks, along with corresponding changes in cerebral perfusion, is particularly crucial for selecting appropriate treatment strategies and providing preventive education. This can significantly improve patient outcomes, reduce mortality, and mitigate disability rates.

This study utilizes 3.0T MRI for high-resolution imaging of carotid artery plaques, aiming to analyze and compare the relationship between ischemic events and plaque burden based on an understanding of plaque composition. Additionally, the study explores the correlation between these factors and cerebral blood flow perfusion parameters (MTT, Average pass time, TTP, Time to peak, CBE, Cerebral blood flow, CBV, Cerebral blood volume). The findings aim to provide effective reference points for the clinical formulation of corresponding treatment plans, preventing adverse cerebrovascular events, and thereby improving the prognosis of a significant number of patients with carotid atherosclerosis.

Materials and methods

Sample information

A total of 40 patients diagnosed with carotid artery plaques through ultrasound examinations conducted at our hospital between July 2021 and August 2022 were selected for inclusion in the study. The ultrasound examinations were performed using GE LOGIQ E9 ultrasound system, which was used to assess the presence of carotid plaques. All patients included in the study were over

18 years of age and provided informed consent prior to participation. Patients were categorized into two groups based on whether the cerebral hemisphere in the carotid artery supply region had experienced ischemic events, including Transient Ischemic Attacks (TIAs): a symptomatic group (16 cases) and an asymptomatic group (20 cases). Basic clinical data were collected for all participants, including age, gender, diabetes, hypertension, hyperlipidemia, coronary heart disease, smoking history, and a history of prior stroke or transient ischemic events. Inclusion criteria were as follows: (1) Patients with good cognitive function who could fully cooperate with the examination; (2) Patients with images that could be diagnostically identified; (3) Patients who had a comprehensive understanding of the project and signed the informed consent form. Exclusion criteria included: (1) Patients with contraindications for magnetic resonance imaging (MRI) examination; (2) Patients with severe consciousness disorders or serious heart, liver, kidney diseases, or tumors; (3) Patients who had previously undergone carotid endarterectomy or stent placement; (4) Patients with extensive lesions such as infarction, softening, deformity, or Fazekas grade 3 (Grading of white matter lesions) white matter hyperintensities (identified in head MRI); (5) Patients with atrial fibrillation; (6) Other conditions deemed unsuitable for participation in the study by researchers, such as pregnant or lactating women, alcoholics, or patients with low compliance due to psychiatric illnesses; (7) Patients with a history of gadolinium contrast agent allergy.

Method

All patients underwent imaging with a Siemens Skyra 3.0T MRI scanner, utilizing a head-neck combined coil along with an 8-channel surface coil. The imaging protocol began with 2D-TOF localization, and MRA images were reconstructed using the MIP method to visualize the position of the carotid arteries. Subsequently, 3D T1 imaging of the carotid arteries was performed using the SPACE sequence (slice thickness: 0.72 mm, TR: 600 ms, TE: 19 ms), covering the proximal segment of the carotid arteries to the range of the middle cerebral arteries. This allowed for precise acquisition of the position, morphology, size, extent, and vascular wall information of carotid artery bifurcation plaques. High-resolution black-blood imaging within a 2 cm range above and below the bifurcation plane was then conducted using T1-weighted imaging (T1WI: TR 708 ms, TE 13 ms), T2-weighted imaging (T2WI: TR 1970 ms, TE 66 ms), and 3D time-of-flight (3D-TOF: TR 21 ms, TE 3.43 ms) sequences, with a slice thickness of 2 mm, a gap of 2 mm, a matrix of 256 × 256, and an FOV of 160 mm × 160 mm (Fig. 1).

Subsequently, gadoteric acid meglumine (0.1 mmol/kg) was injected through the cubital vein at a rate of 3.5–4.0

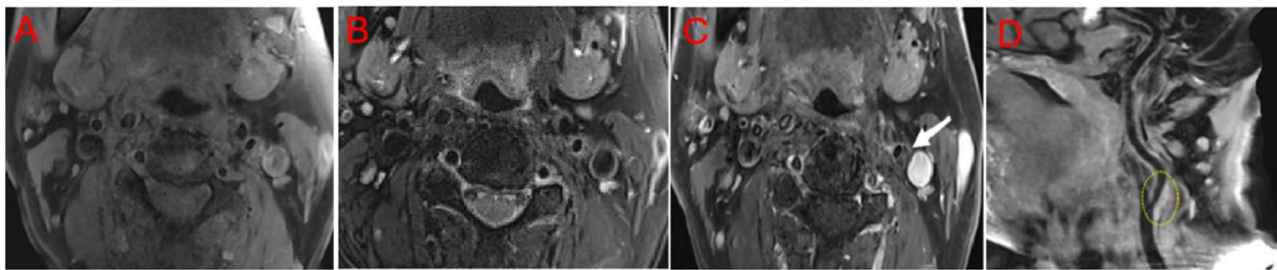


Fig. 1 (A) T1WI, (B) T2WI, (C) CE-T1WI showing the formation of a plaque at the origin of the left internal carotid artery (white arrow). The plaque has a non-enhancing lipid-rich necrotic core, and a continuous enhancing fibrous cap is visible. (D) 3D-SPACE curved surface reconstruction displaying the plaque extent (circle) and the generally slightly thickened vessel wall of the distal internal carotid artery with a patent lumen

mL/s, followed by a saline flush of 20 mL at the same rate. Whole-brain PWI (MR Perfusion Weighted Imaging) (slice thickness: 5 mm, TR: 1600 ms, TE: 30 ms) and carotid artery CE-MRI (T1WI: TR 708 ms, TE 13 ms) were then performed. During the scans, the patient's jaw and head-neck region were immobilized, earplugs were used for hearing protection, and the patient was positioned supine with the head entering the scanner first. Surface coils were snugly placed on both sides of the carotid arteries. Patients were instructed to maintain even and steady breathing and to minimize coughing and swallowing movements. Patients were instructed to maintain even and steady breathing, minimize coughing and swallowing movements, and to keep their eyes closed during the scan to avoid affecting perfusion of the occipital lobe.

Plaque burden and composition statistics

The image data were processed using Siemens post-processing workstations. At the location of the maximum cross-sectional area of the plaque, quantitative measurements of plaque burden were delineated by outlining the measured areas, including luminal area (LA), wall area (WA), total vessel area (TVA), and maximum wall thickness (MaxWT). The normalized wall index (NWI), calculated as $NWI = WA/TVA \times 100\%$, was used to assess plaque burden. Carotid artery luminal stenosis was measured using the North American Symptomatic Carotid Endarterectomy Trial (NASCET) method [3]. This well-established method categorizes stenosis as mild (0–49%), moderate (50–69%), severe (70–99%), or complete occlusion (100%).

Currently, based on a substantial body of literature and experimental data [4], vulnerable plaques are primarily defined as those containing intraplaque hemorrhage (IPH)/neovascularization (AHA VI), lipid-rich necrotic core (LRNC) (AHA IV-V), and plaques with irregular fibrous caps or caps that have ruptured. Therefore, in this study, information on these vulnerable plaque components was also concurrently collected and analyzed.

High-resolution magnetic resonance imaging characteristics of carotid artery plaques

(1) The fibrous cap exhibits a low signal on the TOF sequence and appears relatively equal or slightly higher in signal on the T1WI and T2WI sequences. (2) The lipid-rich necrotic core presents an equal to slightly higher signal on the T1WI and a low to equal signal on the T2WI. (3) The signal of hemorrhagic thrombus is related to the timing of bleeding: recently formed hemorrhagic thrombus shows high signals on both T1WI and T2WI sequences; fresh bleeding thrombus signals high on T1WI and TOF, with unstable signals on T2WI and appearing as equal or low signals; chronic hemorrhage demonstrates low signals on all sequences. (4) Neovascularization within the plaque is markedly enhanced on contrast-enhanced MRI (CE-MRI, T1WI) [5–7].

Analysis of cerebral perfusion images

Utilizing Siemens post-processing workstations, pseudo-color maps of cerebral blood flow perfusion (mean transit time, MTT; time to peak, TTP; cerebral blood flow, CBF; cerebral blood volume, CBV) were generated. Two expert vascular physicians jointly assessed the perfusion images, recording the locations and extents of abnormal perfusion in the brain tissues on the same side as the carotid artery plaque (measured at the level of maximum perfusion abnormality). The following is an analysis of two cases (Figs. 2, 3 and 4).

Case1

A 67-year-old female presented with weakness in the right upper limb. There is a plaque at the origin of the left internal carotid artery, accompanied by a large lipid-rich necrotic core, $NWI = 75.6$, and a stenosis rate of 34. The left temporal-parietal lobe shows elongated MTT and TTP, increased CBV, and no significant change in CBF.

Case2

66 years old, male, admitted for internal examination. Plaque formation at the right internal carotid artery origin, with a large lipid core, $NWI = 86$, stenosis rate of 41.

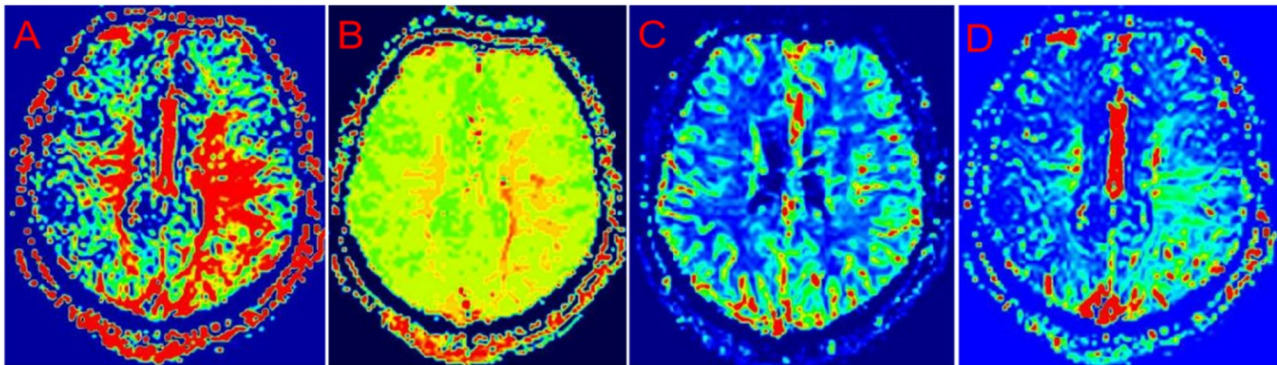


Fig. 2 PWI revealing perfusion abnormalities in the left temporal and parietal lobes: (A) Prolonged MTT, (B) Prolonged TTP, (C) No significant change in CBF, (D) Increased CBV

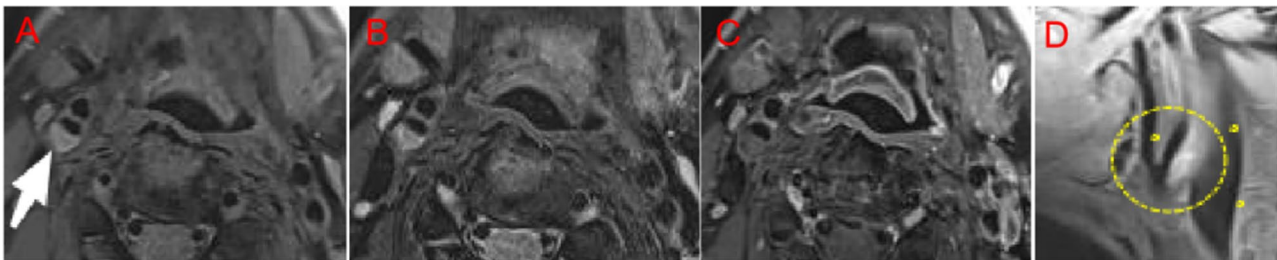


Fig. 3 (A) TIWI, (B) T2WI, (C) CE-TIWI showing the formation of plaque at the right internal carotid artery origin (white arrow), predominantly with a lipid necrotic core and localized inflammatory enhancement. (D) 3D-SPACE reconstruction displaying the plaque and carotid artery bifurcation area (circle)

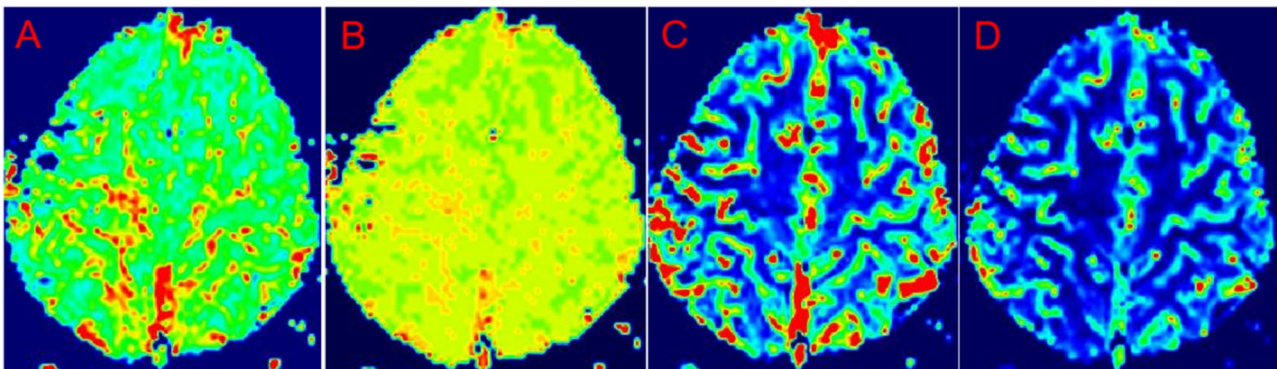


Fig. 4 PWI revealing small patchy perfusion abnormalities in the right parietal lobe: (A) Prolonged MTT, (B) Prolonged TTP, (C) Unremarkable CBF, (D) Increased CBV

Small patchy prolongation of MTT and TTP in the right parietal lobe, with no significant changes in CBV and CBF.

Statistical analysis

Statistical analysis was conducted using SPSS 20.0. Continuous variables are expressed as (mean \pm standard deviation), and the independent samples t-test was employed for comparisons between two groups, while one-way analysis of variance (ANOVA) was used for comparisons among multiple groups. Non-normally distributed data were analyzed using non-parametric tests. Categorical data are presented as percentages and were compared

between groups using the χ^2 test, with $P < 0.05$ considered statistically significant.

Results

Clinical characteristics data of symptomatic and asymptomatic groups

The symptomatic group had an average age of around 61 years, while the asymptomatic group had an average age of around 54 years. The prevalence of hypertension and smokers in the symptomatic group was significantly higher than in the asymptomatic group ($P < 0.05$). However, there were no significant differences in clinical

Table 1 Comparison of clinical characteristics between the two groups ($\bar{x} \pm s, n$)

Group	Age (years)	Hyper-tension (%)	Dia-betes (%)	Hyper-lipid-emia (%)	Smok-ing (%)
Symptomatic group (n=16)	61.13±9.65	37.5	12.5	12.5	25
Asymptomatic group (n=24)	54.88±8.58	0	0	0	0
t/ χ^2	2.147	7.851	-	-	4.178
P	0.038	0.005	0.154	0.154	0.041

The total sample size $N \geq 40$ and the theoretical frequency $1 \leq t \leq 5$, the chi-square test correction formula is used. $T < 1$, the Fisher exact probability method is employed

Table 2 Comparison of burden between two Groups ($\bar{x} \pm s$)

Group	maxWT	NWI (mm2)	Stenosis rate (%)
Symptomatic group (n=16)	4.25(3.875~5.575)	75.6(60~85.5)	35(28.5~39.5)
Asymptomatic group (n=24)	2.5(2.5~2.5)	20(20~20)	10(10~10)
Z	-4.46	-4.701	-4.465
P	0.000	0.000	0.000

The sample does not follow a normal distribution, so non-parametric tests were employed, and the results are presented as medians (25~75%)

Table 3 The composition of LRNC and IPH between two groups

Group	LRNC (%)	IPH (%)
Symptomatic group (n=16)	56.3	50.0
Asymptomatic group (n=24)	16.7	12.5
χ^2	6.857	5.021
P	0.009	0.025

The total sample size $N \geq 40$ and the expected frequency $5 \leq T$, the general formula is used; The expected frequency T is between 1 and 5, the chi-square test correction formula is employed

characteristics such as diabetes and hyperlipidemia between the two groups ($P > 0.05$). Refer to Table 1.

The burden between symptomatic and asymptomatic groups

The symptomatic group exhibited significantly higher values in maxWT, NWI, and stenosis rate compared to the asymptomatic group ($P < 0.05$) Table 2.

The composition between the symptomatic and asymptomatic groups

The incidence rates of LRNC and IPH in the symptomatic group were significantly higher than those in the control group ($P < 0.05$) Table 3.

Table 4 The correlation between blood perfusion parameters and NWI, stenosis

		MTT prolon-gation area	NWI	Ste-nosis rate
MTT prolon-gation area	Pearson Correlation	1	0.653**	0.585*
	Significance (two-tailed)		0.003	0.011
	N	18	18	18
NWI	Pearson Correlation	0.653**	1	0.664**
	Significance (two-tailed)	0.003		0.003
	N	18	18	18
Stenosis rate	Pearson Correlation	0.585*	0.664**	1
	Significance (two-tailed)	0.011	0.003	
	N	18	18	18

** $P < 0.01$, * $P < 0.05$

Reveals a significant correlation between MTT prolongation area and NWI ($P = 0.003$), with a correlation coefficient (r) of 0.653, indicating a significant positive correlation. Furthermore, there is a correlation between MTT prolongation area and stenosis rate ($P = 0.011$), with a correlation coefficient (r) of 0.585, showing a positive correlation. Additionally, NWI and stenosis rate are also correlated ($P = 0.003$), exhibiting a significantly positive correlation with a correlation coefficient (r) of 0.664

Correlation between blood perfusion parameters and NWI, Stenosis

The extent of MTT and TTP prolongation in patients with perfusion abnormalities showed a positive correlation with NWI and stenosis rate. The relationship with NWI was more pronounced, and the differences were statistically significant ($P < 0.05$). Since the MTT and TTP extension ranges were essentially consistent among the study subjects, this study uniformly measured the maximum level of MTT abnormality, as shown in Table 4.

Discussion

In carotid artery plaques patients, performing high-resolution magnetic resonance imaging of the carotid artery (HRMRI) along with whole-brain perfusion one-stop imaging offers a relatively short examination time and the ability to depict plaque morphology, size, composition, and vascular wall burden [8, 9]. Simultaneously, perfusion-weighted imaging (PWI) can provide multiple parameters related to cerebral perfusion, reflecting the extent and severity of cerebral ischemia, serving as a tool for predicting and assessing stroke risk.

Previous studies indicated that hypertension and smoking are risk factors for plaque hemorrhage, while hyperlipidemia is a risk factor for lipid-rich necrotic core [10, 11]. Smokers undergoing carotid endarterectomy had an average age younger by 7 years compared to non-smokers ($P = 0.001$) [12]. In this study, the symptomatic group showed a higher prevalence of hypertension and smoking compared to the asymptomatic group, aligning with previous research. Rots et al. discovered that patients with symptomatic carotid artery stenosis, as evidenced by preoperative MR-DWI showing cerebral ischemia,

were more likely to have intraplaque hemorrhage (IPH), and symptomatic plaques exhibited higher lipid content [13]. This suggests that increased occurrences of IPH and lipid content within plaques are potential indicators of cerebral ischemic risk [14]. In this study, the symptomatic group showed a significantly higher proportion of lipid-rich necrotic core (LRNC) and IPH compared to the asymptomatic group ($P < 0.05$), consistent with previous research findings.

Here, the symptomatic group exhibited a significantly higher Normalized Wall Index (NWI) than the asymptomatic group ($P < 0.05$), and the symptomatic group showed perfusion abnormalities in the carotid artery supply region. Additionally, in all patients with perfusion abnormalities, the range of Mean Transit Time (MTT) and Time to Peak (TTP) was positively correlated with NWI and stenosis rate. The association with NWI was more significant, with statistically significant differences ($P < 0.05$). It has indicated that in stroke patients, the intima-media thickness (IMT) of the carotid artery can serve as an indicator of the clinical severity of ischemic stroke in patients with symptomatic carotid artery stenosis [15]. It has shown that compared to stable plaque groups, the MTT values in the watershed areas of the cortex are significantly prolonged in vulnerable plaque groups, and vulnerable plaques are often relatively thick [16]. In this study, due to the inconsistent degree of dilation at the beginning of the internal carotid artery and varying degrees of shrinkage in the distal internal carotid artery in some patients, it was found that compensatory enlargement of vessel area and lumen area occurred with the continuous progression of plaques. Therefore, plaque size cannot represent the degree of lumen stenosis, and the degree of lumen stenosis cannot reflect the wall burden. NWI can simultaneously represent lumen stenosis and wall thickness [17]. Hence, in this study, the use of NWI to assess carotid artery plaque burden is more accurate [18].

This paper found that some asymptomatic patients also exhibited perfusion abnormalities (prolonged MTT and TTP). The significance of this discovery lies in the fact that asymptomatic patients with perfusion abnormalities may be prevalent in the community. The early cerebral perfusion changes caused by carotid artery plaques have not received sufficient attention. Therefore, this study holds value for community awareness, screening, follow-up, and early prevention of cerebral ischemic events related to carotid artery plaques.

Conclusions

In conclusion, NWI can serve as an indicator for assessing the risk of stroke, providing a basis for early clinical intervention. The higher the NWI, the greater the risk of stroke. The combination of high-resolution carotid vessel

wall imaging and whole-brain perfusion provides valuable references for early clinical intervention.

Limitations

In this study, there are still some limitations. Firstly, it only involves a relatively small sample size due to the advanced age of the patients. Secondly, manual delineation of perfusion areas introduces a certain degree of error, and there was no comparison of perfusion parameter values in the abnormal perfusion areas. Therefore, further research with an increased sample size is needed in the later stages.

Author contributions

The research endeavor represented a collaborative effort, with each author contributing distinct expertise to various aspects of the study. Yonggang Cai played a key role in conceptualization and methodology, while Shouming Chen and Tongyu Shang focused on data curation and investigation. Yonggang Cai and Binze Han took the lead in drafting the original manuscript, and Lei Zhang, Changyan Xu, Zhibin He contributed significantly to the review and editing process. Ting Yin was responsible for visualization and supervision, ensuring the integrity of the research.

Funding

This research was supported by Sichuan Medical Association (Hengrui) Research Fund (2021HR61).

Data availability

The datasets used and/or analyzed during the current study are available from the corresponding author on reasonable request.

Declarations

Human ethics and consent to participate

This study was reviewed and supervised by the Medical Ethics Committee of the Affiliated Hospital of Panzhihua University. (Approval number: 2022223). The study was performed in accordance with the Declaration of Helsinki and the International Conference on Harmonisation Good Clinical Practice guidelines. The protocol and all modifications were approved by relevant ethics committees and regulatory authorities. All patients provided written informed consent.

Clinical trial number

Not applicable.

Competing interests

The authors declare no competing interests.

Received: 30 October 2024 / Accepted: 17 March 2025

Published online: 24 March 2025

References

1. Ge X, Zhou Z, Zhao H, Li X, Sun B, Suo S, et al. Evaluation of carotid plaque vulnerability in vivo: Correlation between dynamic contrast-enhanced MRI and MRI-modified AHA classification. *J Magn Reson Imaging*. 2017;46(3):870–6.
2. Sui B, Gao P. High-resolution vessel wall magnetic resonance imaging of carotid and intracranial vessels. *Acta Radiol*. 2019;60(10):1329–40.
3. Adla T, Adlova R. Multimodality imaging of carotid stenosis. *Int J Angiol*. 2015;24(3):179–84.
4. Seyedasaadat SM, Rizvi A, Alzuabi M, Dugani SB, Murad MH, Huston J 3rd, et al. Correlation of MRI-detected vulnerable carotid plaques with clinical presentation: a systematic review and meta-analysis. *J Neurosurg Sci*. 2020;64(3):263–71.

5. Kotsugi M, Takayama K, Myouchin K, Wada T, Nakagawa I, Nakagawa H, et al. Carotid artery stenting: investigation of plaque protrusion incidence and prognosis. *JACC Cardiovasc Interv.* 2017;10(8):824–31.
6. Brinjikji W, Huston J 3rd, Rabinstein AA, Kim GM, Lerman A, Lanzino G. Contemporary carotid imaging: from degree of stenosis to plaque vulnerability. *J Neurosurg.* 2016;124(1):27–42.
7. Wu F, Yu H, Yang Q. Imaging of intracranial atherosclerotic plaques using 3.0 T and 7.0 T magnetic resonance imaging-current trends and future perspectives. *Cardiovasc Diagn Ther.* 2020;10(4):994–1004.
8. Wei H, Zhang M, Li Y, Zhao X, Canton G, Sun J, et al. Evaluation of 3D multi-contrast carotid vessel wall MRI: a comparative study. *Quant Imaging Med Surg.* 2020;10(1):269–82.
9. Turan TN, Bonilha L, Morgan PS, Adams RJ, Chimowitz ML. Intraplaque hemorrhage in symptomatic intracranial atherosclerotic disease. *J Neuroimaging.* 2011;21(2):e159–61.
10. van den Bouwhuijsen QJ, Vernooij MW, Hofman A, Krestin GP, van der Lugt A, Witteman JC. Determinants of magnetic resonance imaging detected carotid plaque components: the Rotterdam Study. *Eur Heart J.* 2012;33(2):221–9.
11. Song X, Zhao X, Liebeskind DS, Xu W, Zhang J, Wei C, Xu Y, Wang L, Zheng Z, Wu J. Associations between systemic blood pressure parameters and intraplaque hemorrhage in symptomatic intracranial atherosclerosis: a high-resolution MRI-based study. *Hypertens Res.* 2020;43(7):688–95.
12. Wendorff C, Wendorff H, Kuehnl A, Tsantilas P, Kallmayer M, Eckstein HH, Pelisek J. Impact of sex and age on carotid plaque instability in asymptomatic patients-results from the Munich Vascular Biobank. *Vasa.* 2016;45(5):411–6.
13. Horie N, Morofuji Y, Morikawa M, Tateishi Y, Izumo T, Hayashi K, Tsujino A, Nagata I. Communication of inwardly projecting neovessels with the lumen contributes to symptomatic intraplaque hemorrhage in carotid artery stenosis. *J Neurosurg.* 2015;123(5):1125–32.
14. Rots ML, Timmerman N, de Kleijn DPV, Pasterkamp G, Brown MM, Bonati LH, et al. Magnetic resonance imaging identified brain ischaemia in symptomatic patients undergoing carotid endarterectomy is related to histologically apparent intraplaque haemorrhage. *Eur J Vasc Endovasc Surg.* 2019;58(6):796–804.
15. Heliopoulos I, Papaioakim M, Tsivgoulis G, Chatzintounas T, Vadikolias K, Papanas N, Piperidou C. Common carotid intima media thickness as a marker of clinical severity in patients with symptomatic extracranial carotid artery stenosis. *Clin Neurol Neurosurg.* 2009;111(3):246–50.
16. Huo R, Xu H, Yang D, Qiao H, Li J, Han H, et al. Associations between carotid plaque characteristics and improvement of cerebral blood perfusion in patients with moderate to severe carotid stenosis undergoing carotid endarterectomy. *J Magn Reson Imaging.* 2021;53(2):613–25.
17. Cao Y, Sun Y, Zhou B, Zhao H, Zhu Y, Xu J, Liu X. Atherosclerotic plaque burden of middle cerebral artery and extracranial carotid artery characterized by MRI in patients with acute ischemic stroke in China: association and clinical relevance. *Neurol Res.* 2017;39(4):344–50.
18. Che F, Mi D, Wang A, Ju Y, Sui B, Geng X, Zhao X, Zhao X. Extracranial carotid plaque hemorrhage predicts ipsilateral stroke recurrence in patients with carotid atherosclerosis - a study based on high-resolution vessel wall imaging MRI. *BMC Neurol.* 2022;22(1):237.

Publisher's note

Springer Nature remains neutral with regard to jurisdictional claims in published maps and institutional affiliations.